

# Numerical Study on the Effect of Insulator and Wire Mesh Toward Carbon Nanotubes Growth Region in Quasi Pyrolysis Chamber

Chong Jia Yong<sup>1</sup>, Muhammad Amirul Amin Moen<sup>1</sup>, Mohd Fairus Mohd Yasin<sup>1</sup>, Tarit Das<sup>1</sup>, Muhammad Thalhah Zainal<sup>2</sup>, Nurul Adilla Mohd Subha<sup>3</sup> and Norikhwan Hamzah<sup>1\*</sup>

<sup>1</sup>High Speed Reacting Flow Laboratory (HiREF), Faculty of Mechanical Engineering, Universiti Teknologi Malaysia, 81310 UTM Johor Bahru, Johor, Malaysia

<sup>2</sup>Department of Mechanical Precision Engineering (MPE), Malaysia-Japan International Institute of Technology (MJIT), Universiti Teknologi Malaysia, 54100 Kuala Lumpur, Malaysia

<sup>3</sup>Faculty of Electrical Engineering, Universiti Teknologi Malaysia, 81310 UTM Johor Bahru, Johor, Malaysia

\*Corresponding author: [norikhwan@utm.my](mailto:norikhwan@utm.my)

*Submitted 28 February 2025; Revised 19 April 2025; Accepted 24 April 2025; Available online 22 May 2025.*

Copyright © 2025 The Authors.

**Abstract:** Flame synthesis is known to be a more energy- and time-efficient method for producing carbon nanotubes (CNTs) compared to other techniques. However, due to the presence of soot formation and highly oxidizing flame sheet in diffusion flame, synthesized CNT in flame suffers low growth rate and low CNT morphology quality. In this study, feasibility of utilising a quasi-pyrolysis chamber (QPC) with and without wire-mesh at the inlet, located on top of methane diffusion flame which separates the CNT growth region from the flame sheet was numerically simulated. Flame quenching effect by the wire-mesh at the inlet of QPC creating a pyrolysis condition within the chamber with methane flame formed outside the chamber, producing the required high temperature for CNT growth. Furthermore, application of insulator surrounding the flame was also numerically tested to evaluate its effect on temperature distribution within the QPC. The study found that the quasi-pyrolysis condition inside the chamber can be established without using wire-mesh only up to chamber with 12 mm diameter before oxygen starts to seep into the QPC and formed flame inside the chamber. Nevertheless, the temperature increase inside the QPC is minimal with removal of wire-mesh. Besides that, the addition of insulation surrounding the flame has significantly increased the predicted synthesized CNT length by 2.5 times. This is due to the increment of CO concentration more than 3 times inside QPC with application of insulator. Consequently, higher CO concentration helps to enhance the CNT growth region within the QPC from initially confined to the region near to the inlet of QPC, to all areas within the QPC. Hence, to ensure high energy efficiency and robustness, utilization of QPC with wire-mesh and insulator should be incorporated in the future development of practical CNT synthesis process in flame.

**Keywords:** Carbon nanotubes; Computational fluid dynamics; Flame synthesis; Insulator; Quasi-pyrolysis chamber.

## 1. INTRODUCTION

Carbon Nanotubes (CNTs) were first discovered in 1991, and the first reported synthesis of single-walled carbon nanotube was reported by Iijima and Ichihashi in 1993 [1]. Since then, CNTs synthesis process has been rapidly developed by researchers, and its utilization is found in various applications for the last three decades due to its remarkable electrical, thermal, and mechanical properties. There are various methods of synthesizing CNT such as chemical vapor deposition (CVD), arc discharge method, laser ablation method, and flame synthesis. Among these methods, flame synthesis is theoretically the most energy- and time-efficient method as hydrocarbon flame can offer both the carbon source and the heat source needed for CNT synthesis [2].

Generally, the working principle of flame synthesis involves the reaction between fuel (hydrocarbon) and oxidizer (oxygen from air) which produces a gaseous mixture including carbon dioxide (CO<sub>2</sub>), water vapor (H<sub>2</sub>O), carbon monoxide (CO), hydrogen (H<sub>2</sub>), saturated and unsaturated hydrocarbons and radicals. In previous related works, CO is found to be the main carbon precursor for CNT growth on catalyst nanoparticles based on transition metals such as nickel, iron, and cobalt [3, 4]. The catalyst nanoparticles may be exposed in flame through substrate or in vapor form to produce carbon nanostructures [5]. There are number of flame configurations used in CNT synthesis such as premixed, counter-flow diffusion, co-flow diffusion, and inverse diffusion flame which has been found to be able to produce CNT at various rates [6].

Diffusion flame is found to be suitable for producing CNT at the center of the flame, with the flame sheet providing the suitable temperature and incomplete combustion at the upstream of the flame providing the required carbon precursor (8). However, CNT growth region in diffusion flame is confined within a highly oxidizing flame sheet located at the outer region of a diffusion flame causing damage to the synthesized CNTs [7]. Furthermore, the most practical growth method for CNT in flame is using vapor type catalyst, where the catalyst nanoparticles float into the flame environment, rich with carbon sources at high temperature, suitable for CNT growth [8]. Hence, the catalyst nanoparticles are within the growth region in less than a second as it floats from the burner outlet to the flame sheet caused by the buoyancy effect of the flame, limiting the feasibility of producing long CNT strands [8]. Previous related works on diffusion flame CNT synthesis have mostly focused on the feasibility analysis and morphology of the synthesized CNTs and has yet to explore method to lengthen the CNT growth region within the diffusion flame.

In recent work, a novel implementation of a quasi-pyrolysis chamber (QPC) is proposed to enhance the growth and quality of CNTs synthesized in a diffusion flame while significantly improving the practicality of the synthesis process by enabling longer CNT growth for vapor-based catalyst [9]. The proposed method utilizes cylindrical tube QPC placed on top of diffusion flame with wire mesh at the inlet to provide flame quenching effect, creating an oxygen free pyrolysis region inside the QPC, with high concentration of carbon precursor. The QPC enables separation of flame sheet from the CNT growth region at the middle of diffusion flame, allowing for longer period of CNT growth within the chamber and away from the highly oxidizing region of the flame sheet. The formation of diffusion flame is limited to the outside the chamber provides the required heat to ensure the inside region of the chamber is at a high temperature required for the CNT synthesis process to occur [9]. However, the current setup of the QPC is prone to heat loss as most of the heat produced by the diffusion flame is wasted on the surroundings, hence creating a low efficiency synthesis process. Furthermore, even though the application of wire mesh at the inlet of the chamber is found useful to quench flame formation, it also minimizes the mass flow rate of carbon precursor into the QPC, hence limiting the maximum the CNT growth rate and growth region [10].

By combining computational models at both the flame and particle levels, it is possible to predict catalytic CNT growth during flame synthesis with high accuracy, reducing the need for extensive experimental work to validate CNT growth processes in flame [10]. The two main models employed in flame synthesis simulations are flame-scale models and particle-scale models [8, 11]. Flame-scale models focus on the chemical kinetics of combustion, which involve studying the reactions that occur during the combustion process, including the formation and development of flames. These models analyze factors such as reaction rates, species concentrations, and temperature distributions, providing a comprehensive understanding of the complex chemistry in flames and how they interact with different fuels and oxidizers [12]. On the other hand, particle-scale models, also known as molecular dynamics simulations, simulate the interactions and behavior of individual atoms or molecules at the nanoscale. Zainal et al. introduced the Growth Rate Model (GRM) to predict CNT growth in a flame environment [13]. GRM is based on specific assumptions about the interactions between catalyst particles and the carbon source. It assumes that catalyst particles cannot maintain their surfaces intact enough to prevent CNT growth. Additionally, methane is considered the primary carbon source in the two-step reaction outlined in the GRM. To simplify the model, the GRM disregards any energy gained from base expansion, thus eliminating the impact of catalyst particle lifting. Moreover, GRM does not take into account the competition between soot particles and other forms of carbon nanomaterials [13]. Nevertheless, this model provides valuable insights into the structural and mechanical properties of CNTs by including factors such as carbon atom diffusion into catalyst nanoparticles, CNT nucleation, and catalyst deactivation within the flame environment.

The present study numerically investigates the impact of thermal insulator and wire mesh application toward the CNT growth rate and distribution of CNT growth region in methane diffusion flame using the QPC. The CFD simulation of flame formation and temperature distribution inside the chamber is validated using experimental data. Results from the CFD simulation are then used as input for the GRM model to predict the CNT growth rate and growth region distribution with the QPC. The result from the work will provide fundamental understanding to improve the cost and energy-efficiency of the QPC based CNT synthesis process and enhance its practicality for broader industrial application in the future.

## 2. EXPERIMENTAL PROCEDURE

A schematic diagram of a methane diffusion flame burner with a synthesis chamber is shown in Figure 1. In this study, a computational fluid dynamics (CFD) reacting flow model is developed to simulate the formation of methane diffusion flame at the actual burner outlet. A two-dimensional axisymmetric model is utilized to represent the chamber with the burner outlet located 20 mm from the inlet of the QPC. In addition, the methane gas and dry air are to flow from the inner and outer annuli of the burner respectively. The flow rate of methane and oxidizer are 0.4 slpm and 3.7 slpm respectively. The validation of the developed diffusion flame with QPC model is carried out using experimental data collected using the identical burner available in High Reacting Flow (HiREF) Laboratory in Universiti Teknologi Malaysia. The modelled diffusion flame is validated using the temperature and visual observation of the standing flame. Temperature measurement of the QPC centerline at various height was captured using bare wire B-type thermocouple with 0.5 mm bead size, attached to a single-axis actuator. Temperature data are taken when the QPC is with and without wire mesh.

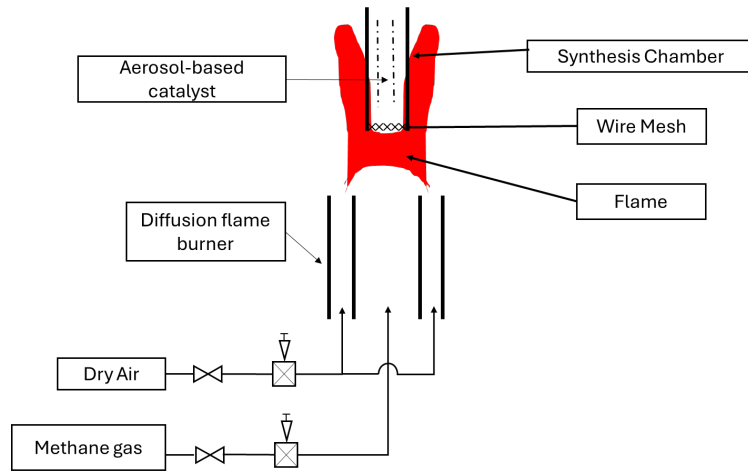


Figure 1. Schematic diagram of the methane diffusion burner with a QPC.

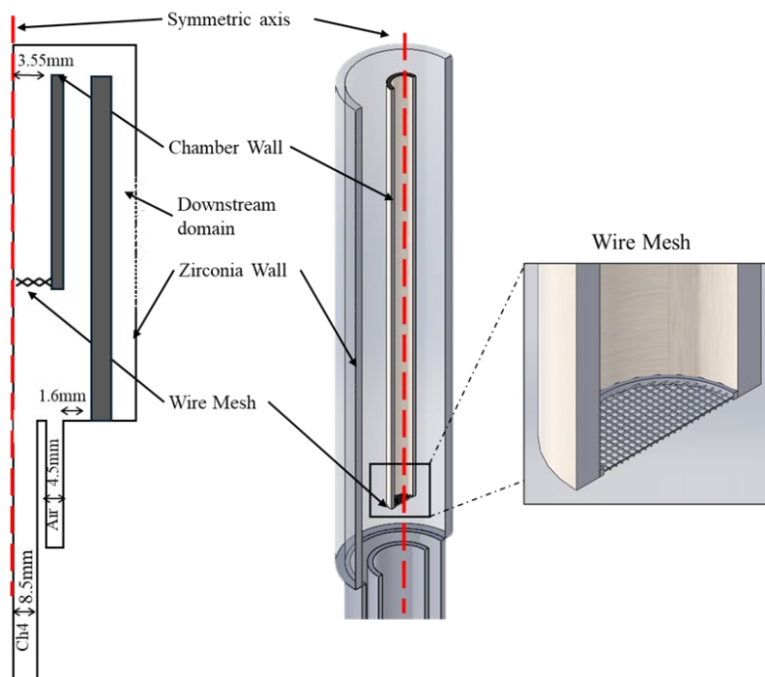


Figure 2. Schematic diagram(left) and 3D section view visualization (right) of the methane diffusion burner with Zirconia insulator.

In this study, numerical analysis is done using a combination of second-order discretization schemes and the Green-Gauss cell-based gradient reconstruction to ensure high accuracy [14]. For the pressure field, a second-order scheme was chosen to reduce numerical diffusion and improve the fidelity of pressure-related calculations. Momentum, turbulent kinetic energy, turbulent dissipation rate, energy, and mean mixture fraction equations were all discretized using second-order upwind schemes, balancing accuracy and computational cost by considering flow direction and capturing the effects of turbulence and scalar quantities more precisely [15]. Additionally, the energy equation was activated to account for heat transfer, and the standard k-epsilon turbulence model with standard wall functions was employed to model turbulence effects. The P1 radiation model was used to simulate radiative heat transfer, and the non-premixed combustion model was utilized to accurately represent the chemical reactions occurring in the system. These discretization choices and model selections were made to achieve a high level of accuracy while maintaining computational efficiency, reducing numerical errors, and providing precise simulations of the physical phenomena under investigation. However, the simulated model did not include presence of catalyst vapor inside methane gas flowing from the fuel side of the burner. Besides reducing calculation load, the data required by the GRM model does not require catalyst related data from the simulated model.

Removal of wire mesh from the inlet of the QPC will enable higher carbon precursor flow rate into the chamber and promote higher CNT growth rate. Nevertheless, the removal of wire mesh is limited to the maximum allowable diameter of the synthesis chamber which enables quasi-pyrolysis condition within the chamber. To evaluate the feasibility and the effect of removing wire mesh from the inlet of the synthesis chamber, the wire mesh blocks are removed from CFD geometry.

Formation of the flames were identified through analysis of temperature distribution throughout the simulated region. Effect of chamber diameter toward the flame formation and temperature distribution were analyzed to identify the optimized diameter of the chamber without utilization of wire mesh.

To simulate the effect of insulator, Zirconia based insulator has been selected as the best insulation material with low thermal conductivity, 2.7 W/mK and relatively very high melting point of 3430 K. Practicality of the material selected is important especially for high-temperature applications as the highest temperature of the methane-diffusion flame could reach up to 2000K [19]. The inner diameter of the insulator is set to be the same as the outer diameter of the burner to give the best insulation effect toward the flame and synthesis chamber with no gap between the synthesis chamber and the burner as visualized in Figure 2. The thickness of the insulator is fixed at 2.5 mm which is identical to off-the-shelf insulator commonly used in combustion work within the HiREF laboratory.

The synthesized CNT length which represents the growth rate and the growth region distribution inside the chamber are simulated using a the GRM model which requires input from the CFD simulation on the temperature and mass fractions of species within the chamber [16]. There are several simplifying assumptions that were incorporated in the GRM to enable the model to focus on the key mechanisms influencing CNT growth. First, catalyst particles are assumed to not undergo surface splitting which may inhibit CNT formation, is excluded from the simulation. Second, methane was assumed to be the primary carbon source driving the two-step reaction pathway. Third, a base-growth mechanism was considered, neglecting any energy gain from the lifting of catalyst particles to simplify the energy balance. Additionally, potential competition between soot formation and the growth of other carbon nanomaterials was also not taken into account [17]. With these assumptions, as mentioned earlier, the GRM does not require simulation data on the catalyst availability within the chamber to simulate CNT growth. Hence, to reduce the simulation complexity, aerosol-based catalyst which is used in the actual test rig is not included in the CFD model to avoid multiphase simulation works.

### 3. RESULTS AND DISCUSSION

#### 3.1 Model Validation

The developed model is validated using two different experimental data set from the actual experimental test rig, standing methane diffusion flame with and without QPC. First, flame shape validation was performed by visual comparison of the simulated model with experimental data as shown in Figure 3. The simulated flame front, defined by a stoichiometric mixture fraction of 0.0622 which represented by the blue line on the temperature contour, closely matched with the experimental flame location. Both the simulated and experimental flame heights were in good agreement, and the radial flame extents were within approximately 10 mm of the burner centerline. This strong agreement validates the model's predictive capability with respect to flame shape for a standing methane diffusion flame.

To ensure validity of the simulated model with presence of QPC, the temperature distribution of the simulated model is compared to the temperature data at the region near to the chamber inlet indicated as T1 to T3 in Figure 4. For validation work, the chamber inlet is fixed at 20 mm HAB and the temperature measurements were made at 10, 15 and 20 mm above the inlet wire mesh as shown in the same figure. It is crucial for the model to be able to predict closely the temperature within this region since this is where most of the growth of CNT is expected to occur. The percentage error between the simulated temperature and the experimental data is found to be less than 15% which is reasonable due to the complexity of reactive flow simulation [20, 21]. Besides that, the simulated model able to replicate the flame structure engulfing the synthesis chamber as per visual observation of the established flame in Figure 4. Furthermore, from temperature contour visualization, the model developed did not produce any flame formation within the chamber as expected. With the model validated, a CFD model of the baseline setup for the CNT synthesis process using QPC in methane diffusion flame is established.

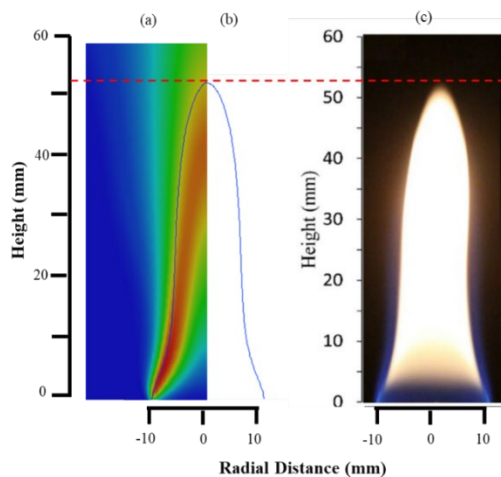


Figure 3. Comparison of flame shape of standing flame of CFD and experiment, (a) simulation flame, (b) iso-line of stoichiometric mixture fraction, (c) experimental flame.

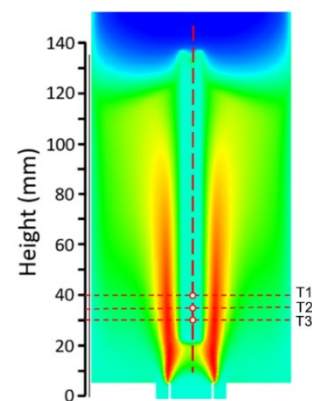


Figure 4. The simulated model of methane diffusion flame with QPC at 20 mm HAB. The dotted lines indicate the location of temperature measurement at the centre of synthesis chamber.

### 3.2 Effect of Inlet Wire Mesh and QPC Diameter

Even though the application of wire mesh at the inlet of the QPC will be able to ensure formation of quasi-pyrolysis environment within the chamber, the presence of wire mesh redistributes the flow at the inlet of the chamber and redirect flame flow field to the outer side of the QPC at the inlet of the chamber. Using the established baseline CFD model, the temperature contour comparison upon the removal of the wire mesh from the chamber inlet can be referred to in Figure 5. It is clear, at the same chamber diameter, the flame does not enter the synthesis chamber even though the wire mesh has been removed, which means that the QPC is still valid even without wire mesh. Furthermore, this result reflects the actual observation made using the experimental test rig which validates the accuracy of the simulation model.

To evaluate the advantages of removal of the wire mesh, temperature plots of the chamber centerline from the inlet to outlet for both simulations were compared as shown in Figure 6. At the inlet of the chamber, the centerline temperature of the chamber is significantly higher compared to the inlet temperature with wire mesh. This is due to the absence of flame-quenching effects at the inlet by wire mesh. This positive effect however is not observed at the other part of the synthesis chamber. Even though an overall temperature increase is observed throughout the chamber centerline, the difference of temperature is minimal, ranging only around 20 to 80 °C, which is relatively insignificant to contribute toward any changes of CNT growth region within the QPC [22, 23]. The minimal increment in temperature may not provide strong justification for wire mesh removal since the presence of wire mesh provides a robust method in preventing formation of flame inside the chamber in case of any instability of the flame throughout the synthesis process. Nevertheless, from the experimental work, it was found that the presence of wire mesh at the inlet of QPC will produce amorphous carbon buildup on the wire mesh overtime. Reduction in the porosity of the wire mesh due to the amorphous carbon will force redistribution of the flame flow field at the inlet of the QPC to the outside of the QPC and reduce the gas mass flow rate into the QPC. Hence, even though removal of wire mesh does not contribute toward higher temperature gains inside the QPC, it will enable a much more uniform and higher gas flow rate into the QPC to provide more consistent synthesis process.

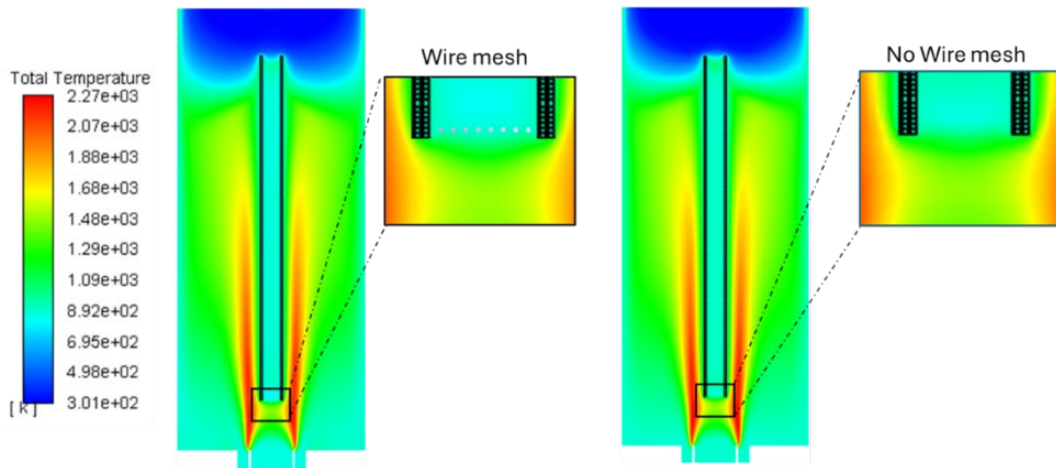


Figure 5. Temperature contour comparison with (left) and without (right) wire mesh at the inlet of synthesis chamber.

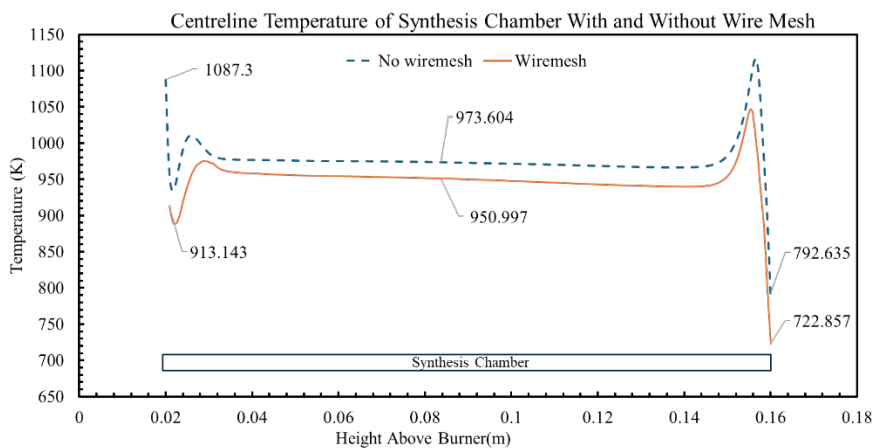


Figure 6. Temperature contour comparison with (left) and without (right) wire mesh at the inlet of synthesis chamber.

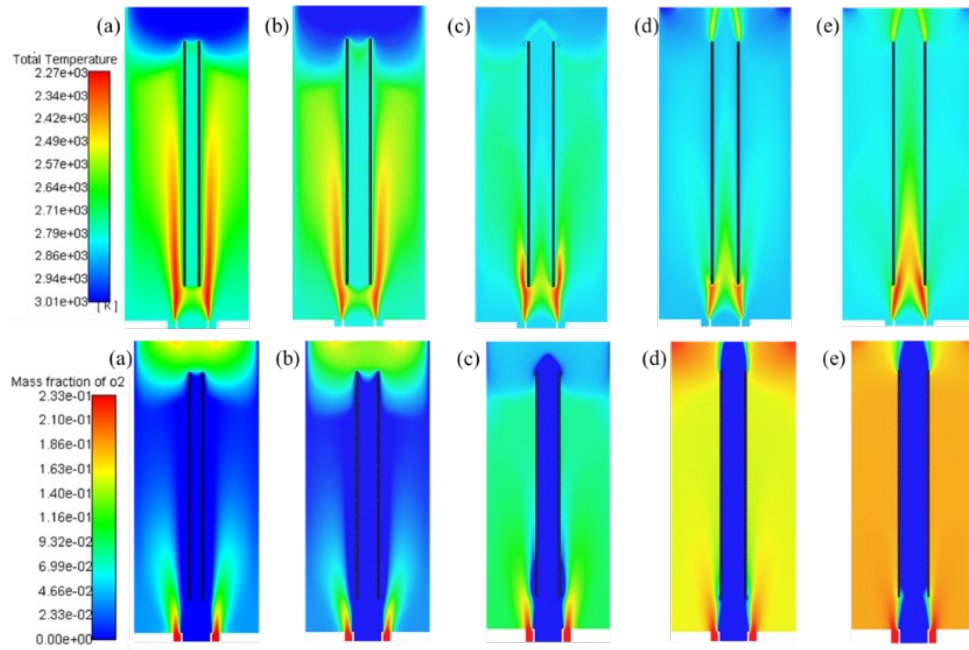


Figure 7. Temperature (top) and oxygen (bottom) contour of synthesis chamber without wire mesh with diameter of (a) 7 mm (baseline model), (b) 12 mm, (c) 13 mm, (d) 14 mm, (e) 17 mm. The dark lines represent the synthesis chamber wall.

To analyze the maximum diameter of the chamber without wire mesh, the diameter of the QPC is increased in the simulation until the flame enters the chamber as shown in Figure 7. The results indicate that partial quasi-pyrolysis condition can be maintained inside the QPC without wire mesh up to 12 mm diameter. When the QPC diameter is 13 mm, the diameter of the QPC is larger than the fuel side of the burner. Hence, redirection of the flame flow field at the burner outlet is minimal without presence of wire mesh, initiating partial flame formation on the inside which indicated by the presence of high temperature region at the inlet of the QPC as shown in top row of Figure 7. Flame quenching effect at the QPC inlet still occurs even without wire mesh at a smaller QPC diameter as the flame has direct contact with the colder wall of the synthesis chamber which tends to absorb heat energy from the flame, lowering its temperature and preventing flame formation inside the chamber. However, this effect is significantly reduced as the chamber diameter increases allowing formation of flame inside the chamber.

The second row of Figure 7 shows an increasing concentration of oxygen outside the QPC at diameters of 7 mm to 17 mm indicates decreasing amount of methane for combustion process. With small QPC diameter than the burner outlet, significant amount of methane is redirected toward the outside of the QPC, producing flame formation close to the inlet. However, as the QPC diameter increases, it was observed that oxygen concentration at the outer region of the QPC is increasing due to the significant reduction of the fuel. Since the methane gas flow from the middle of the burner, with larger chamber, most of the fuel flow straight to the chamber without being redirected to the outside of the QPC. Nevertheless, these results apply specifically to a chamber HAB of 20 mm and the baseline flame flow rate; any changes to these parameters may shift the maximum allowable diameter for maintaining quasi-pyrolysis without wire mesh. This result clearly shows the importance of wire mesh to ensure quasi-pyrolysis condition inside QPC at higher diameter which may be applicable for large scale CNT production in the future.

### 3.3 Effect of the Application of Insulator and Insulator Thickness

It is expected that application of insulator surrounding the QPC will help to concentrate the heat distribution toward the QPC and maximize the utilization of heat produced from the methane diffusion flame toward the synthesis process. From the temperature contour comparison for process with and without insulator in Figure 8, it can be clearly seen that the flame formation with an insulator is more stable and produces longer flame compared to the baseline model. Without the insulator, the baseline model shows that the flame propagates away from the wall of the chamber downstream of the burner. With the insulator, the flame formation is more restricted and directed more concentratedly towards the synthesis chamber causing lesser heat loss to the surroundings. Furthermore, the insulator also inhibits the cooling effect of the cool surrounding air that entrapped into the flame due to buoyancy effects. Temperature-wise, the centerline temperature inside the chamber has increased between 20 to 80K, while the temperature at the outer domain has dropped from 1177.29K to 1097.71K proving that heat loss to the surrounding from the wall of the chamber has been reduced.

To evaluate the effect of insulator toward the CNT growth rate, GRM model is utilized to simulate the CNT growth inside the chamber, with and without wire mesh and insulator. In the GRM simulation result, it is assumed that no CNT is produced if the predicted length of the CNT is shorter than 1  $\mu\text{m}$ . Based on GRM simulation results in Figure 9, the maximum CNT length produced for all models is located at the inlet of the chamber. This is because this location has the maximum temperature and abundance of carbon sources for CNT growth. Interestingly, the GRM result predicted that chamber with and without wire mesh shows have minimal difference in term of maximum CNT length and growth region. The CNT growth region is expected

to be concentrated only around less than 10 mm near to the inlet of the chamber, with or without wire mesh. However, the addition of insulator increases the maximum CNT length from 24.67  $\mu\text{m}$  to 85.4  $\mu\text{m}$  which is a 2.5-fold increase. Furthermore, the CNT growth region also expands to cover the entire synthesis chamber, representing a 4.7-fold enhancement over the baseline model. The significant difference of the growth rate and growth region distribution can be explained through analysis of methane ( $\text{CH}_4$ ) and carbon monoxide ( $\text{CO}$ ) mass fraction within the chamber with the presence of insulator.

Figure 10 shows the contour map of  $\text{CH}_4$  and  $\text{CO}$  mass fraction for setup with and without insulator. Comparison of the contour map from the simulation results clearly shows the importance of insulator in diverting more  $\text{CH}_4$  toward the inside the synthesis chamber, while high temperature ensures that higher concentration of  $\text{CO}$  is available inside the chamber due to pyrolysis process. As one of the main carbon precursors for CNT growth, the presence of high  $\text{CO}$  will directly promote much higher CNT growth rate inside the chamber. Hence, the CNT growth is predicted throughout the length of the chamber by the GRM model as the concentration of  $\text{CO}$  remains elevated throughout the chamber.

Figure 11 below shows detailed analysis of  $\text{CH}_4$  and  $\text{CO}$  mass fraction radial distribution at 30mm height above burner. Interestingly,  $\text{CH}_4$  is not present at this height inside the chamber without insulation which indicates minimal concentration at the inlet of the QPC. This is mainly due to the redirection of the flame field flow at the inlet of QPC which causing the majority of the fuel flow is distributed to the outer region of the chamber. Without insulator to limit the spatial distribution of the flame flow field, the fuel mixes with the surrounding air and further minimizes the heat generated from the combustion process which can be seen from the temperature and flame length comparison in Figure 8 previously. Whereas, with availability of insulator, more  $\text{CH}_4$  is directed to inside of the chamber and contributed to the growth of CNT as carbon precursor. The  $\text{CO}$  concentration is also elevated with the pyrolysis process of methane with the presence of higher temperature when insulator is in place.

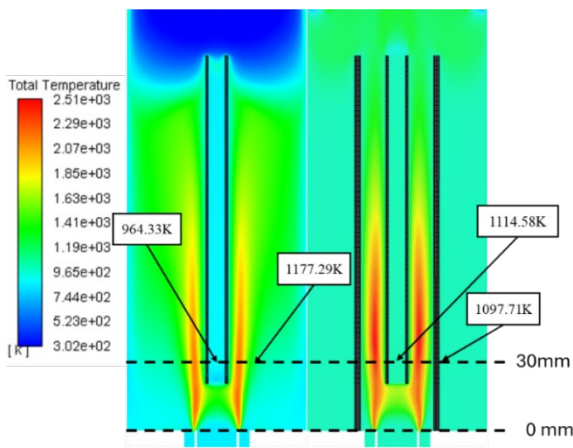


Figure 8. Temperature contour comparison without (left) and with (right) Zirconia insulator. Inner and outer dark lines represent the chamber wall and insulator wall respectively. The temperature data collected at 30 mm above burner.

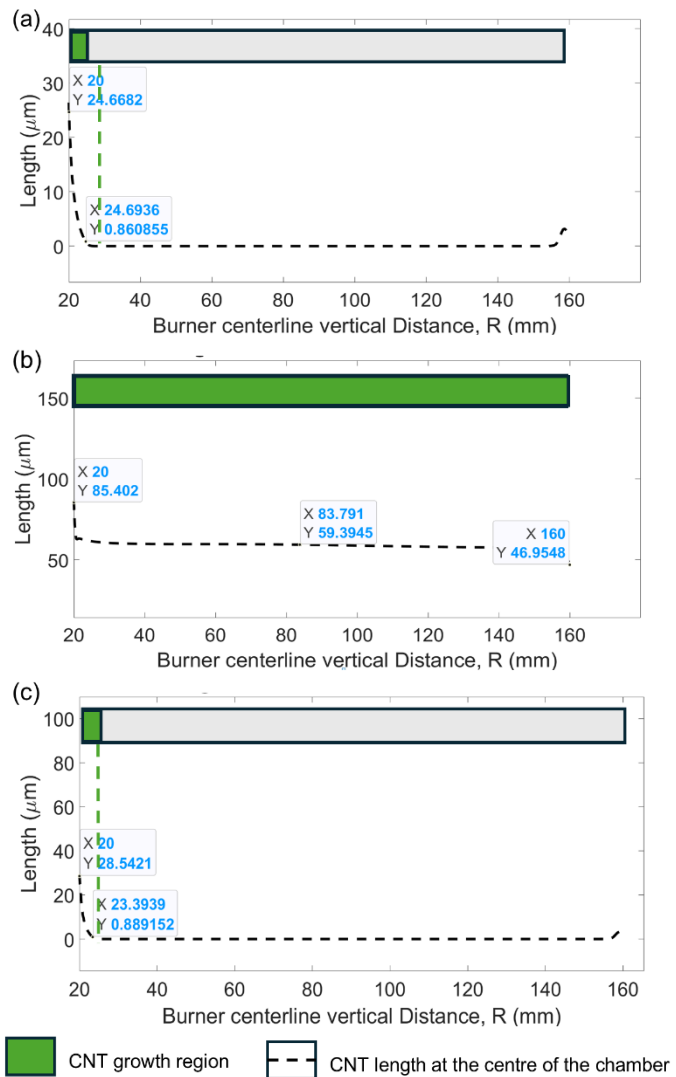


Figure 9. CNT length and growth region at the centerline of synthesis chamber (a) baseline model, (b) baseline model with 2.5 mm insulator, (c) baseline model without wire mesh.

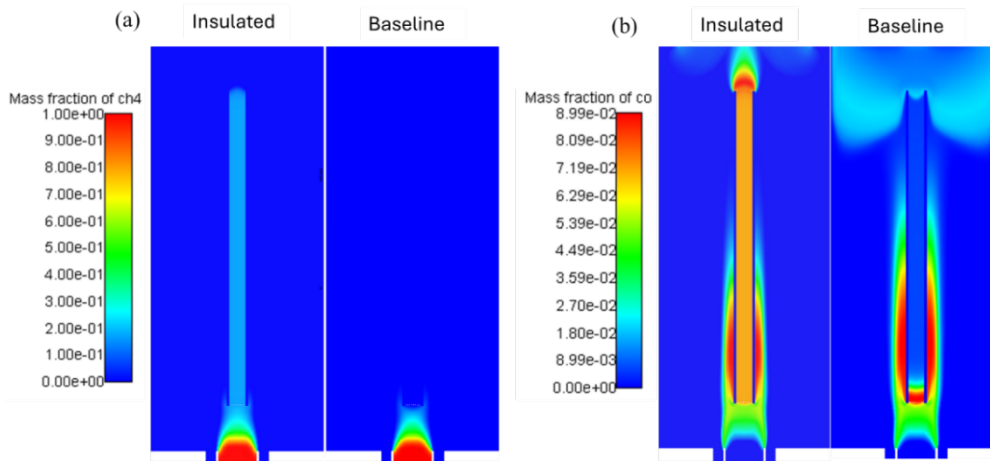


Figure 10. Contour plot of (a) CH<sub>4</sub> and (b) CO concentration with and without (baseline) insulator.

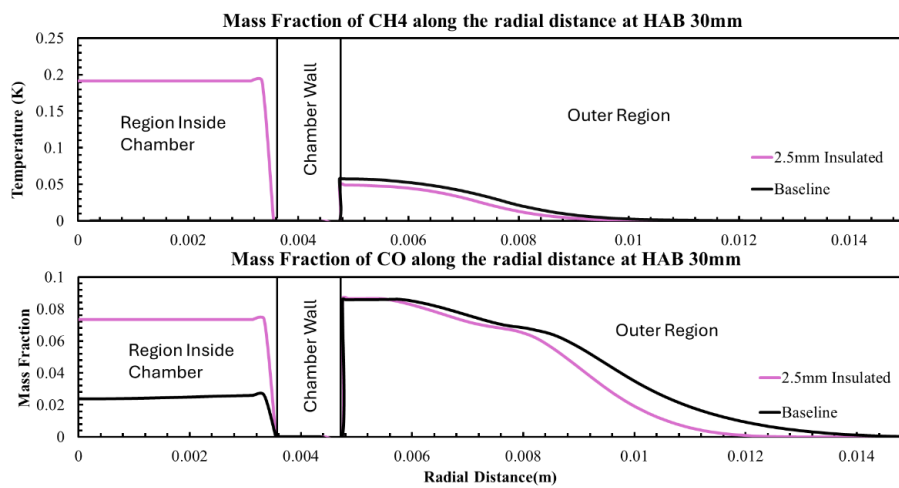


Figure 11. Mass fraction of CH<sub>4</sub> and CO along the radial distance at HAB 30 mm for baseline model and insulated model. The bar in the middle shows the region of the data taken at HAB 30 mm.

Even though CH<sub>4</sub> and CO mass fractions inside the chamber significantly increase with addition of insulator, wire mesh presence does not visibly change the concentration of CH<sub>4</sub> at the inlet and throughout the chamber as shown in Figure 12(a) contour map. However, the CO coverage region of the wire mesh model is slightly higher in the synthesis chamber as shown in Figure 12(b). This explains the slightly longer CNT growth region predicted by the GRM simulation in the baseline model with 24.69 mm for chamber with wire mesh compared to 23.39 mm predicted by the GRM for the model without wire mesh. The slightly longer maximum CNT length observed in the model without wire mesh may be due to the higher temperature in the synthesis chamber upon wire mesh removal as no heat energy is absorbed by wire mesh leading to a more conducive environment for CNT growth [24].

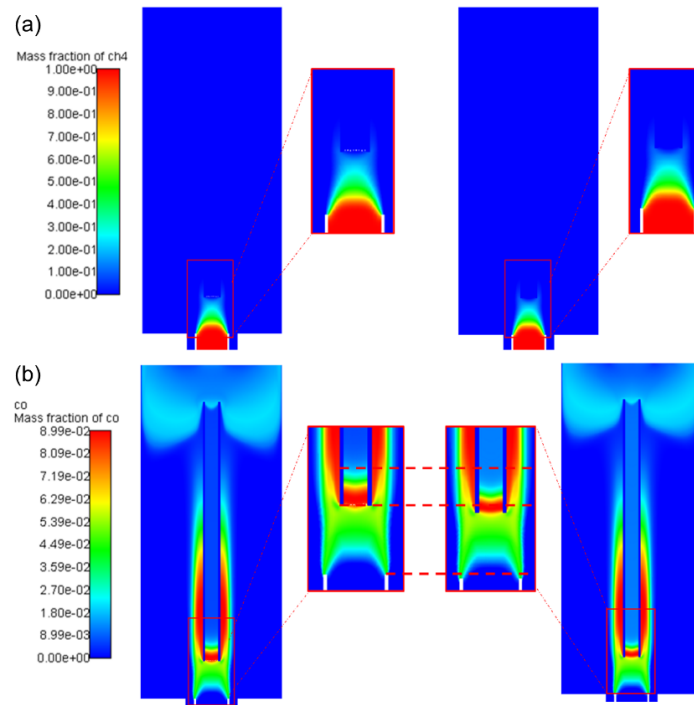


Figure 12. Contour map of (a) CH<sub>4</sub> and (b) CO concentration for synthesis chamber with (left) and without (right) wire mesh. Red dotted lines are to indicate the height of CO inside the chamber.

#### 4. CONCLUSION

This study has numerically investigated the impact of thermal insulation and wire mesh application on the CNT growth rate and growth region distribution using a quasi-pyrolysis chamber (QPC) placed above a methane diffusion flame. The developed CFD and GRM models were successfully validated with experimental data, confirming the accuracy of the predicted flame structure and temperature distribution within the QPC. The findings demonstrate that while the wire mesh effectively maintains a quasi-pyrolysis condition by preventing flame formation inside the chamber, its removal leads to only a minimal increase in temperature, insufficient to significantly enhance CNT growth. However, removing the wire mesh improves gas flow uniformity and reduces potential flow restrictions due to carbon build-up on the mesh, offering a more consistent synthesis environment. The study further identified that a maximum QPC diameter of 12 mm can sustain quasi-pyrolysis conditions without wire mesh; beyond this, oxygen infiltration and internal flame formation occur, necessitating wire mesh use for larger-scale chambers for practical application in the future. More significantly, the addition of thermal insulation around the QPC was shown to substantially improve CNT growth performance. The insulated setup increased the maximum CNT length by 2.5 times and expanded the growth region by 4.7 times compared to the baseline. This enhancement is attributed to better heat retention, improved flame stability, and higher CO concentration inside the chamber due to increased CH<sub>4</sub> pyrolysis efficiency. The elevated CO levels throughout the QPC played a pivotal role in promoting CNT growth along the full length of the chamber. Overall, this study provides strong evidence that integrating both wire mesh and thermal insulation in QPC-based CNT synthesis setups can optimize energy utilization, stabilize flame dynamics, and significantly enhance the growth rate and spatial distribution of CNTs. These insights contribute valuable guidance for the future design and scaling of efficient and robust flame-based CNT synthesis systems for industrial applications.

#### ACKNOWLEDGMENT AND FUNDING

The authors would like to acknowledge the financial support from Ministry of Education Malaysia under Fundamental Research Grant Scheme (FRGS) (FRGS/1/2022/TK09/UTM/02/7) and Universiti Teknologi Malaysia for the funding under UTM Fundamental Research grant (UTMFR) (Q.J130000.3824.23H99).

#### DECLARATION OF CONFLICTING INTERESTS

The authors declare no potential conflicts of interest with respect to the research and publication of this article.

#### REFERENCES

- [1] S. Rathinavel, K. Priyadharshini and D. Panda, A review on carbon nanotube: An overview of synthesis, properties, functionalization, characterization, and the application, *Materials Today: Proceedings*, 45, 2021, 5316-5322.
- [2] W. Merchan-Merchan, A. V. Saveliev, L. Kennedy and W. C. Jimenez, Combustion synthesis of carbon nanotubes and related nanostructures, *Progress in Energy and Combustion Science*, 36(6), 2010, 696-727.
- [3] Y. H. Tang, Y. F. Zheng, C. S. Lee, N. Wang, S. T. Lee and T. K. Sham, Carbon monoxide-assisted growth of carbon nanotubes, *Chemical Physics Letters*, 342, 2001, 259-264.

- [4] A. G. Nasibulin, A. Moisala, D. P. Brown and E. I. Kauppinen, Carbon nanotubes and onions from carbon monoxide using  $\text{Ni}(\text{acac})_2$  and  $\text{Cu}(\text{acac})_2$  as catalyst precursors, *Carbon*, 41, 2003, 2711-2724.
- [5] H. Chu, W. Han, F. Ren, L. Xiang, Y. Wei and C. Zhang, Flame synthesis of carbon nanotubes on different substrates in methane diffusion flames, *ES Energy & Environment*, 2, 2018, 73-81.
- [6] N. Hamzah, M. F. M. Yasin, M. Z. M. Yusop, A. Saat and N. A. M. Subha, Rapid production of carbon nanotubes: A review on advancement in growth control and morphology manipulations of flame synthesis, *Journal of Materials Chemistry A*, 5, 2017, 25144-25170.
- [7] N. Hamzah, M. F. M. Yasin, M. Z. M. Yusop, M. A. S. M. Haniff, M. F. Hasan, K. F. Tamrin and N. A. M. Subha, Effect of fuel and oxygen concentration toward catalyst encapsulation in water-assisted flame synthesis of carbon nanotubes, *Combustion and Flame*, 220, 2020, 272-287.
- [8] Y. Mo, H. Zhou, B. Zhang, X. Du, Z. Lin, W. Li, H. Y. Liu and Y. W. Mai, Facile flame catalytic growth of carbon nanomaterials on the surface of carbon nanotubes, *Applied Surface Science*, 465, 2019, 23-30.
- [9] C. Weise, A. Faccinetto, S. Kluge, T. Kasper, H. Wiggers, C. Schulz, I. Wlokas and A. Kempf, Buoyancy induced limits for nanoparticle synthesis experiments in horizontal premixed low-pressure flat-flame reactors, *Combustion Theory and Modelling*, 17, 2013, 504-521.
- [10] M. T. Zainal, M. F. Mohd Yasin, M. Abdul Wahid and M. Mohd Sies, A flame structure approach for controlling carbon nanotube growth in flame synthesis, *Combustion Science and Technology*, 193, 2021, 1326-1342.
- [11] R. Waelder, C. Park, A. Sloan, J. Carpena-Núñez, J. Yoho, S. Gorsse, R. Rao and B. Maruyama, Improved understanding of carbon nanotube growth via autonomous jump regression targeting of catalyst activity, *Carbon*, 228, 2024, 119356.
- [12] E. Blurock and F. Battin-Leclerc, Modeling combustion with detailed kinetic mechanisms, *Green Energy and Technology*, Springer, 2013, 17-57.
- [13] S. Naha, S. Sen, A. K. De and I. K. Puri, A detailed model for the flame synthesis of carbon nanotubes and nanofibers, *Proceedings of the Combustion Institute*, 31(II), 2007, 1821-1829.
- [14] M. T. Zainal, M. Fairus, M. Yasin, M. Abid, I. Irawan, M. F. Roslan, N. Hamzah, M. Zamri and M. Yusop, Investigation on the deactivation of cobalt and iron catalysts in catalytic growth of carbon nanotube using a growth rate model, *Journal of Advanced Research in Materials Science*, 51, 2018, 11-22.
- [15] P. Młynarczyk, The influence of the numerical solver selection on the nozzle impulse flow simulation results, *MATEC Web of Conferences*, 240, 2018, 03008.
- [16] K. Fukumoto and Y. Oka, Simulation of turbulent non-premixed and partially premixed, *Journal of Thermal Science and Technology*, 9(1), 2014, 1-13.
- [17] K. J. Kim, W. R. Yu, J. H. Youk and J. Lee, Factors governing the growth mode of carbon nanotubes on carbon-based substrates, *Physical Chemistry Chemical Physics*, 14, 2012, 14041-14048.
- [18] W. Guanghai, S. Haoran, W. Chunpeng, Z. Jian, H. Yanli, Z. Shichao and C. Yufeng, High temperature microstructural evolution of  $\text{ZrO}_2$  fibers thermal insulation materials, *Key Engineering Materials*, Trans Tech Publications Ltd, 2014, 319-322.
- [19] L. S. Tao, Y. F. Chen, S. C. Zhang, K. W. Deng, H. R. Sun, X. K. Sun, D. C. Yan, K. Fang and N. Li, Preparation and performance of zirconia fiber board, *Solid State Phenomena*, Trans Tech Publications Ltd, 2018, 912-917.
- [20] Y. Jaluria, Use of experimentation in the accurate numerical simulation of thermal processes, *WIT Transactions on Engineering Sciences*, 2010, 241-252.
- [21] D. V. Krasnikov, S. N. Bokova-Sirosh, T. O. Tsendsuren, A. I. Romanenko, E. D. Obratsova, V. A. Volodin and V. L. Kuznetsov, Influence of the growth temperature on the defective structure of the multi-walled carbon nanotubes, *Physica Status Solidi B: Basic Research*, 255(1), 2018, 1870101.
- [22] M. H. Ibrahim, N. Hamzah, M. Z. M. Yusop, N. L. W. Septiani and M. F. M. Yasin, Control of morphology and crystallinity of CNTs in flame synthesis with one-dimensional reaction zone, *Beilstein Journal of Nanotechnology*, 14, 2023, 741-750.
- [23] M. Li, Z. Xu, Z. Li, Y. Chen, J. Guo, H. Huo, H. Zhou, H. Huangfu, Z. Cao and H. Wang, An experimental and CFD study on gas flow field distribution in the growth process of multi-walled carbon nanotube arrays by thermal chemical vapor deposition, *Crystal Research and Technology*, 51, 2016, 702-707.
- [24] Y. C. Yue, W. Ren, M. L. Zhao, M. X. Guo, Y. T. Zhang, J. Xia and D. J. Li, Effect of reaction temperature on carbon nanotubes, *Advanced Materials Research*, 2011, 1383-1386.